



## Assessment of Rock Engineering Risk Management Frameworks Used in Underground Mines

Simbarashe Geja,<sup>1</sup> Maidei Meck<sup>2</sup>, and Desire Runganga<sup>2</sup>

<sup>1</sup> Dept. of Mining Engineering, University of Zimbabwe. Harare, Zimbabwe

<sup>2</sup> Minerals to Metals Initiative, University of Cape Town, South Africa

### KEYWORDS

*Rock engineering  
Fall of ground  
Rock-mass  
Risk  
Geotechnical*

### ABSTRACT

Over 40% percent of the accidents encountered at Unki Mines are related to ground failure and other geotechnical complications. This research sought to address the monetary losses incurred in revenue and productivity through absenteeism and injury. With the development of mine production in Zimbabwe, the depth of mines gradually increased, and the ecological environment developed complex conditions. Deep mining unlike shallow mining is characterized by extra ground pressure, more gas, and faster deformation rates. These factors affect the safety of mining production. Therefore, as the mining depth and breadth increase, the difficulty of mine rock engineering is also increasing. The deepening of mining depth and the improvement of the mechanization level have brought increasing difficulties regarding the stability of surrounding rock hence risk issues arise. The ultimate objective of this study was to ensure a robust design of support systems at Unki Mine that would eventually reduce the risks associated with rock engineering excavations. Findings from the study and its analysis established the following conclusions. On the fore is the fact that hanging wall instability at Unki Mine are predominantly governed by geological and span attributes. The computed k value is 7% less the k value of 57.33 MPa used for existing pillars. An analysis of FOS and its relationship with recovery and Pillar W/H ratio shows that over-break has a huge impact on the span stability hence the effect of the ANFO need to be reviewed for an alternative explosive that ensures recovery within 80% range to ensure that the FOS is maintained above 1.6. A decrease in FoS increases the probability of failure, hence it is also important to device a pillar support system that is less prone to effects of over-break since the ground conditions are poor.

### ARTICLE HISTORY

*Received 8 May 2023  
Received in revised form  
26 June 2023  
Accepted 30 August 2023  
Available online 11 September  
2023*

© 2023 The Authors. Published by Pentract Technology.

This is an open access article under the CC BY-NC 4.0 license (<https://creativecommons.org/licenses/by-nc/4.0/>).

## 1. INTRODUCTION

The demands on rock engineering are increasing for the purposes of mineral extraction, energy and civil structures. Many of the new rock structures being proposed are novel and without precedent, for example, the storage of high-level nuclear waste in underground repositories. Others need to be constructed within stiff environmental and safety constraints and within tighter financial budgets without the spiraling and escalating costs so frequent in many of today's rock engineering projects. The desire to optimize any part of the rock engineering will be restricted by the constraints imposed. Constraints cover a wide and diverse range of criteria and can include such as factors as location, shape and dimension of the engineering

structure, financial limits, contractual arrangements, and time limits for each stage of the works, expertise and personnel available and possibly political and ethical considerations. The objectives and constraints essentially constitute the degree of flexibility in which the project can operate and can be the project management boundary conditions. [1][2].

## 2. BACKGROUND

The high incidence of workplace accidents in the mining sector continues to be a problem for mining and quarrying executives [3]. Risk assessment and management approaches are most often used in subterranean engineering projects using

\*Corresponding author:

E-mail address: Desire Runganga<[desirerunganga@gmail.com](mailto:desirerunganga@gmail.com)>.

<https://doi.org/10.56532/mjsat.v3i3.161>

2785-8901/ © 2023 The Authors. Published by Pentract Technology.

This is an open access article under the CC BY-NC 4.0 license (<https://creativecommons.org/licenses/by-nc/4.0/>).

a qualitative or semi-quantitative approach. In general, a risk register is created, which identifies the risk events that may be associated with the project in each of several disciplinary fields (such as geotechnical or rock engineering); the likelihoods and consequences of each of these risk events; the control, counter, and mitigation measures that are planned or required to be put in place; and the residual risks that may exist after the project has been implemented. Risks linked with occurrences such as rock bursts, major deformations, collapses, karst, water inrushes, and weak rock would usually be noted in such a risk register. The results might include a variety of economic and non-economic repercussions on the project, such as those listed in. [4][5].

Environmental management systems and processes are critical for major mining operations like Unki to achieve both a good image and a safe environment. As a result, it's crucial to figure out how risk management policies are applied in both direct and indirect activities. Mines has put in place a framework that lays out its risk management processes. It adheres to the NOSA Integrated Five Star system, which is maintained by the National Occupational Safety Association (NOSA) and incorporates three key elements: safety, health, and the environment.[6] The risk management assessment will help in finding long lasting solutions for mines in Zimbabwe. Both modes involve creating economic value from knowledge packaging and offer further benefits to the state universities by way of access to successful industry CEOs to serve as student mentors, as well as industrial exposure and experience that further enrich their research and teaching staff. Rock engineering risk are taken seriously in Zimbabwe, and the country's legislative system encourages ecologically responsible mining practices. The Mines and Minerals Act, which governs the mining sector, is primarily governed by the Ministry of Mines and the Chamber of Mines. Environmental concerns in mining, according to the BMI (2010), are addressed at the project inception and development stage by the Environmental Management Agency. The Environmental Management Act, Chapter 20:27 of 2003, is the primary tool for environmental management. This thesis is concerned with the development of a methodology to guide the rock engineering process

Over 40% percent of the accidents encountered at Unki Mines are related to ground failure and other geotechnical complications. This research seeks to address the monetary losses incurred in revenue and productivity through absenteeism and injury. With the development of mine production in Zimbabwe, the depth of mines gradually increased, and the ecological environment developed complex conditions. Deep mining unlike from shallow mining is characterized by extra ground pressure, more gas, and faster deformation rates [7][8]. These factors affect the safety of mine production. Therefore, as the mining depth and breadth increase, the difficulty of mine rock engineering is also increasing.

The deepening of mining depth and the improvement of the mechanization level have brought increasing difficulties regarding the stability of surrounding rock hence risk issues. In addition, the mining influence leads to exposure of weak rock surfaces to stress in the process of excavation and artificial disturbance, and then extends micro and macro cracks, until the whole rock mass is destroyed. The destroyed rock mass would

cause the instability of surrounding rock and supporting problem, and bring about a series of environmental disasters, such as rock burst, mine roadway roof caving, impact ground pressure, or surface subsidence. These environmental disasters will seriously affect the safe production of mining enterprises. To solve these geotechnical complications and ground failures, a comprehensive extension method should be proposed.[9][10]

To reduce these environmental disasters in mines, the safety assessment and hazard identification is important in the process of mine operations. Meanwhile, reliable excavation and supporting could be provided by scientific and reasonable evaluation of the surrounding rock. As the premise of support, assessment of the effectiveness of the risk management and hazard identification applied in rock engineering projects in underground mines is an urgent problem to be solved at Unki mine given the nature of geotechnical complications characterizing the mine. The research sought to assess Risk management framework on ground failure at Unki Mine and ascertain optimal design methodology of underground engineering excavations under high stress and weak geotechnical conditions at Unki.

### 3. METHODOLOGY

The Fuzzy logic taxonomic analysis of risks was employed to identify the root causes of rock engineering accidents and provide future direction for corrective measures to reduce the probability of occurrence of the event. A fuzzy logic system was used to model the cause-and-effect relationships, assess the degree of risk exposure and rank the key risks in a consistent way. Accessing the mine safety reports database (FOG incidents). Available information was organized using taxonomic analysis principles followed by creation of a taxonomic scheme consisting of 5 layers/taxons and application of fuzzy logic model to improve risk assessment and risk decision making.[11]

#### 3.1 FOG statistics

The Unki FOG statistics were deliberated on fully in order to define the ground support requirements. The Unki Mine FOG database was used filter irrelevant incidents to this research such as FOG prompted by conveyor belt suspended weights. The height of potential fall in a rock mass is the most critical parameter that influence support design. The fall-out heights were determined from in-situ measurements of dislodged rocks after falls. statistics on influence of geology on FOG were also incorporated to establish which rock engineering properties of geological structures had the most influence on FOG. These statistics also sought to establish how certain mining tasks prompt FOG hence statistics on the frequency of FOG during certain Tasks was analyzed. The rationale of all this was that it would control the framework of the engineering solutions against FOG and other hazards emanating from rock engineering properties. [12][13].

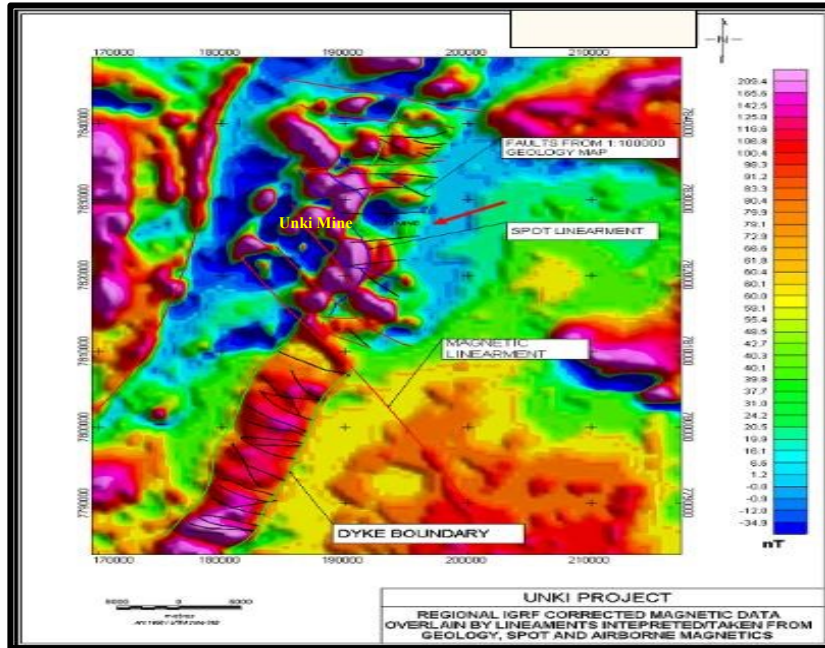


Fig. 1. Aeromagnetic image showing faults around Unki Mine

3.2 Geotechnical Mapping

Major discontinuities inclusive of dykes, faults and joints were mapped using in some instances survey pegs; small distinctively labeled metallic discs secured on the hanging wall at known X, Y, and Z coordinates acting as reference points from which mapping originated. A 60m soft tape was first fixed, taut, between two points and the distance of each discontinuity: from the peg and to the face as well as trace length was recorded using soft tape and a distometer. All discontinuity contacts were recorded where they cut across the Base of the Main Sulphide Zone BMSZ line. Measurements were done on both sides of the side walls; the true dip of each structure was under examination and combined into the CADSMINE Software to update the geotechnical maps.

3.3 Rock Engineering-Based Risk Management

The research followed an extensive analysis of laboratory test work of rock engineering properties at Unki Mine. The research placed emphasis on analyzing results from the following test.

3.4 Uniaxial Compression Strength, UCS Tests

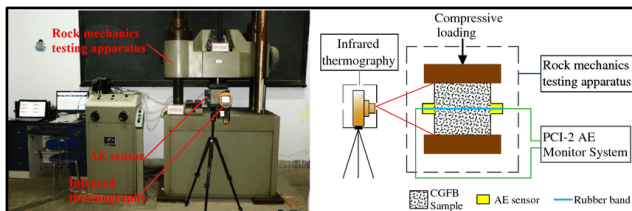


Fig. 2. Procedure for UCS test modified from Zhao & Chunlai 2019.

Using results from this test, it was possible to analyze the strength of a rock mass or determine the UCS of a rock sample. The test was used for characterizing intact rock or determining the strength of any excavations to be made, whether surface- or underground. Ryder and Jager (2002) propose that a sample

of cross-sectional area (A) is loaded with an increasing force (F) until it fails. The peak stress (F/A) at failure is known as the unit cell stress (UCS) and can be represented by the symbol QC. Besides measuring the axial load, strain rosettes or gauges bonded to the specimen vertically and horizontally are also used to measure axial and radial strains or deformations. During the test, the stress-versus-strain curve for the axial and lateral directions is plotted. Failure occurs within five to ten minutes [14]. To calculate the tangent or secant elastic modulus, the average slope of the stress-strain curve is used. The compressive strength,  $\sigma_c$  is computed as indicated in the following equation:

$$\sigma_c = F / A \tag{1}$$

Where, F is the compressive force on the sample or highest load, A is the preliminary cross-sectional area, In this test process, compressive stresses and strains are deemed positive [15]. Axial strain,  $\epsilon_a$ , is considered as indicated below:

$$\epsilon_a = \Delta l / l_0 \tag{2}$$

Where:  $\Delta l$  is the variation in determined axial length,  $\Delta l_0$  is the axial length of specimen before loading. Radial strain is defined either by determining the variations in specimen diameter or by determining the circumferential strain [16]. In the instance of determining the variations in diameter, the radial strain,  $\epsilon_d$  is computed as indicated below:

$$\epsilon_d = \Delta d / d_0 \tag{3}$$

Where:  $\Delta d$  is the change in diameter (negative for an increase in diameter)  $d_0$  is the diameter of the specimen prior to loading. The Young's modulus, E, of the rock is defined as the ratio of the change in axial stress to the change in axial strain as shown in the following equation.

$$E = \sigma \varepsilon \alpha \quad (4)$$

Poisson's ratio ( $\nu$ ) is the “absolute value of the ratio of the diametric or transverse strain to the axial strain in compressive loading” [17] and is calculated as shown below:

$$\nu = \left| \frac{-\text{radial strain}}{\text{axial strain}} \right| \quad (5)$$

### 3.5 Brazilian Tensile Tests



Fig. 3(a). Brazilian Test

Two metal loading jaws are outlined to contact a disc fashioned rock specimen at diametrically opposed surfaces over an arc of contact. The rate at which the specimen was loaded was set ensuring failure in 5 minutes. A loading rate of 200 N/s was used. The specimen is loaded to failure and is assessed for mode of failure. At least 10 test samples are needed [17][18][19]. The results were recorded, and the indirect tensile strength of the sample was computed as follows.

$$\sigma_t = \frac{2F}{\pi LD} \quad (6)$$

Where F = Load at failure  
L = Length of sample(mm)  
D = Diameter of sample (mm)  
Triaxial compressive strength tests

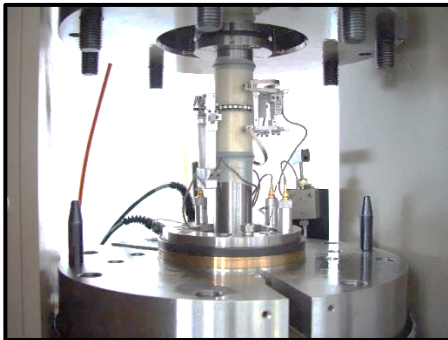


Fig. 3(b). Triaxial Compressive test

Tests of triaxial strength are done to determine the strength of cylindrical rock specimens subjected to triaxial compression. Triaxial strength tests simulate underground rock behavior by determining the strength of cylindrical rock specimens subjected to triaxial compression. Minor stress was

applied around the curved surface by the fluid pressure through the synthetic rubber jacket when the Amsler testing machine was used on the cylindrical-shaped rock sample [21][22]. Triaxial strength tests use the same sample preparation methods as UCS tests, which are described in previous sections. Confining pressures of 5, 10, 15, 20 and 25 MPa were used consecutively in order to determine the strength at which the sample fails. The pressure at Unki Mine underground conditions was considered because the orebody dips at 140.

The increase in depth also intensifies the stress and influences the rock strength. For triaxial strength test, the sample was overloaded axially at a stable rate so that failure happens in 5 minutes. The weight was discharged completely, keeping the axial pressure larger than radial pressure to avoid breaking the synthetic rubber jacket and the above step was repeated for all the samples. The results are plotted on an Axial Pressure ( $\sigma_1$ ) vs Confining Pressure ( $\sigma_3$ ) graph over the range of confinement. The results are plotted on an Axial Pressure ( $\sigma_1$ ) vs Confining Pressure ( $\sigma_3$ ) graph over the range of confinement. Where an almost linear strengthening correlation was established on a  $\sigma_1$  vs  $\sigma_3$  space, the values of the  $\sigma_1$  intercept  $\sigma_c$  and slope  $B_0$  were read off. The angle of internal friction  $\phi$  and cohesion  $C_0$  were calculated from the following equations according to Ryder (2002).[23][24][25]

$$\sigma_1 = \sigma_c + \beta_0 \sigma_3 \quad (7)$$

$$\beta_0 = \frac{1 + \sin \phi_i}{1 - \sin \phi_i} \quad (8)$$

$$\sin \phi_i = \frac{\beta_0 - 1}{\beta_0 + 1} \quad (9)$$

$$\phi_i = \arcsin \frac{\beta_0 - 1}{\beta_0 + 1} \quad (10)$$

$$C_0 = \frac{\sigma_c (1 - \sin \phi_i)}{2 * \cos \phi_i} \quad (11)$$

Where:  $\beta_0$  is the computed gradient of the line of best fit and  $\sigma_c$  is its y-intercept.

### 3.6 Rock Mass Classification

Common rock mass classification systems inclusive of RQD, Q, RMR and Laubscher's MRMR systems were employed to classify the rock mass. At selected localities relevant geotechnical parameters that influence the performance of the rock mass were measured and recorded. These included: joint set number, joint spacing, joint roughness, joint infill type, joint infill thickness, orientation of discontinuities and ground water conditions. The joint volumetric count (JV) method suggested by Palmström (1982) was employed to establish the RQD rating [26][27][28]. The value of JV was first computed by means of the joint spacing per interval using the following expression.

$$J_V = \frac{1}{J_1} + \frac{1}{J_2} + \frac{1}{J_3} \quad (12)$$

Where J1, J2, J3 are joint sets 1, 2 and 3 respectively. For purposes of rock engineering risk management, the rock mass classification was employed to; Evaluate the impact of ground conditions on underground rock engineering stability; Establish quantitative data and rock engineering guidelines for geological excavations. The research employed MRMR values in carrying out computations of rock mass strength (RMS) adjusted obtain design rock mass strength (DRMS), the k value useful in pillar strength and factor safety computations.[29]

$$W_{eff} = 4 \left[ \frac{ab}{a+b+c+d} \right] \tag{13}$$

The heights ha, hb, hc and hd establish the effective height of each pillar as given by.

$$h_{eff} = \left[ \frac{ah_a + bh_b + ch_c + dh_d}{a+b+c+d} \right] \tag{14}$$

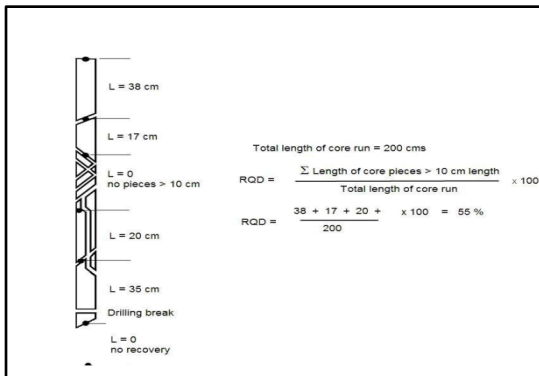


Fig. 4. Procedure for measuring and Calculation of RQD[30]

3.7 Support Appraisal and Design

Pillar measurements and observations were used to facilitate computations of pillar stress. Pillar failure as triggered by poor ground conditions or design deficiencies were examined together with their instantaneous and long-term impacts.

3.8 Factor of Safety

The Hedley and Grant method for establishing average pillar strength was employed, by measuring the dimensions a, b, c and d as illustrated to define the effective pillar width by the tributary area method.[31]

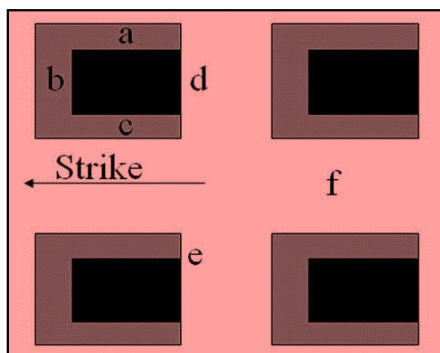


Fig. 5. Measured Pillar Dimensions for the Hedley and Grant method

Effective pillar width (weff) was established based on the following.

3.9 DRMS based on Laubscher’s Mining Rock Mass Rating (MRMR) Classification System

An underground plan superimposed with the surface plan was employed to define depths below surface at various points of the mine. The depth below surface (z) at a point underground was found by calculating the difference between the elevation of the surface contour at that point and the peg elevation. Areal extraction ratio for each pillar was also determined using the formula suggested by Brady & Brown, 1985. After determination of depth below surface as well as areal extraction ration, the average pillar stress was then calculated. After finding the pillar stresses and pillar strength, factors of safety for pillars under study were calculated.

3.10 Span Stability

The modified stability graph method suggested by (Potvin, 1988) and (Nickson, 1992) was applied to assess the pillar and span design at the mine. For the determination of the Q’ value of the section, Q-system data produced for each bord was averaged. Potvin factor analysis was done in each bord in the specific areas where the Q-system of rock mass rating had been done. The modal Potvin factor values were used to calculate the modified stability number N’ of the section which was then used to determine the stable unsupported hydraulic radius in the section.

4. RESULTS

The methods highlighted above were used to derive, analyze, and discuss various findings to come up with the results analyzed under this section. The section shows the results established on the relation of FOG incidents and their geological root causes, appraisal results for the support system and proposed designs.

The analysis shows that rock mass failure resulted in just below 50% of FOG at the mine, support failure caused 26% FOG incidents and human interactions accounted for the extra 24%. It may be deduced therefore that were rock mass structures have been accounted for, engineering controls to manage FOG seem to be effective. Efforts to detect rock mass abnormalities and human interactions with support systems is critical in reinforcing the rock engineering risk management systems.

4.1 Pillar Factor of Safety

Pillar FOS is typically used at Unki mine as a measure for ensuring geotechnical safety within rock engineering excavations. The Pillar FOS was calculated using the equation given below with variations of the value of  $k$  ( $k_1=57.3$  and  $K_2=DRMS=53.2$ ) used for computing  $Q_{Ave}$

$$FOS = \frac{Q_{Ave}}{Q_p} \tag{15}$$

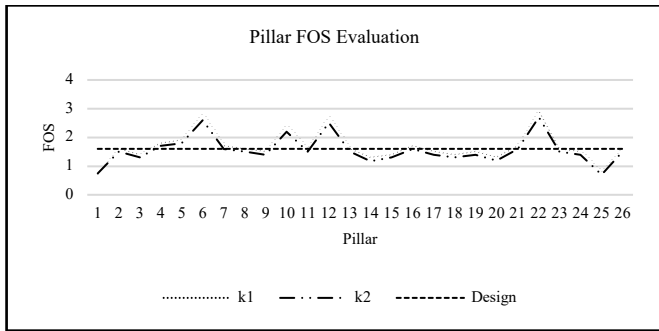


Fig. 6. Pillar FOS

It above figure shows that the determined DRMS/  $k$  value of 53.2 MPa yielded FOS values below a  $k$  value of 57.33MPa. A  $k$  value of 53.3MPa had a least FOS of 0.7 and a peak of 2.9 and a mean of 1.5 which is below design.

4.2 Pillar FOS and W/H Ratio

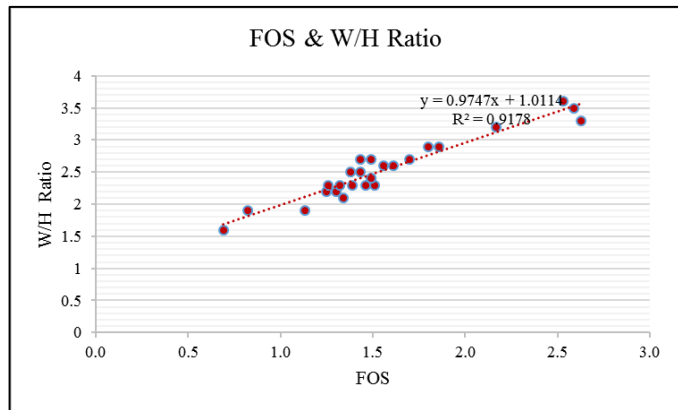


Fig. 7. Pillar strength and Width to height ratio

The figure above indicates a strong positive correlation between width to height ratio and the pillar strength as evidenced by the correlation coefficient 0.92. The greater the width to height ratio the higher the pillar strengths and FOS.

4.3 FOS and Recovery

The below figure clearly shows proof of a strong negative correlation between the extraction ratio and the pillar FOS evidenced by a correlation coefficient  $R^2=0.95$ . Empirical evidence such as the tributary area theory proposes that the extraction ratio rises as the FOS falls due to the rise in pillar stress.

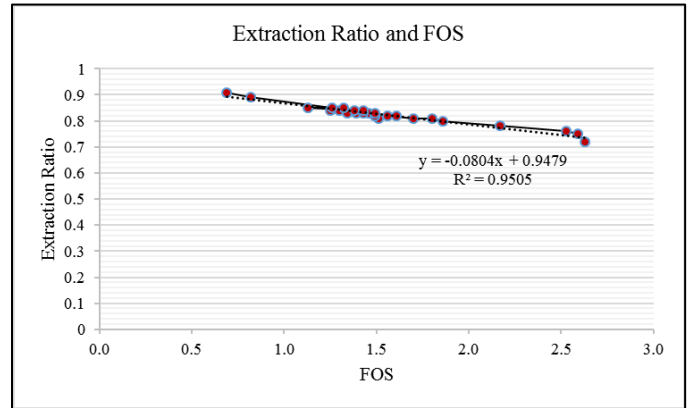


Fig. 8. Extraction Ratio and FOS

4.4 Structural Mapping

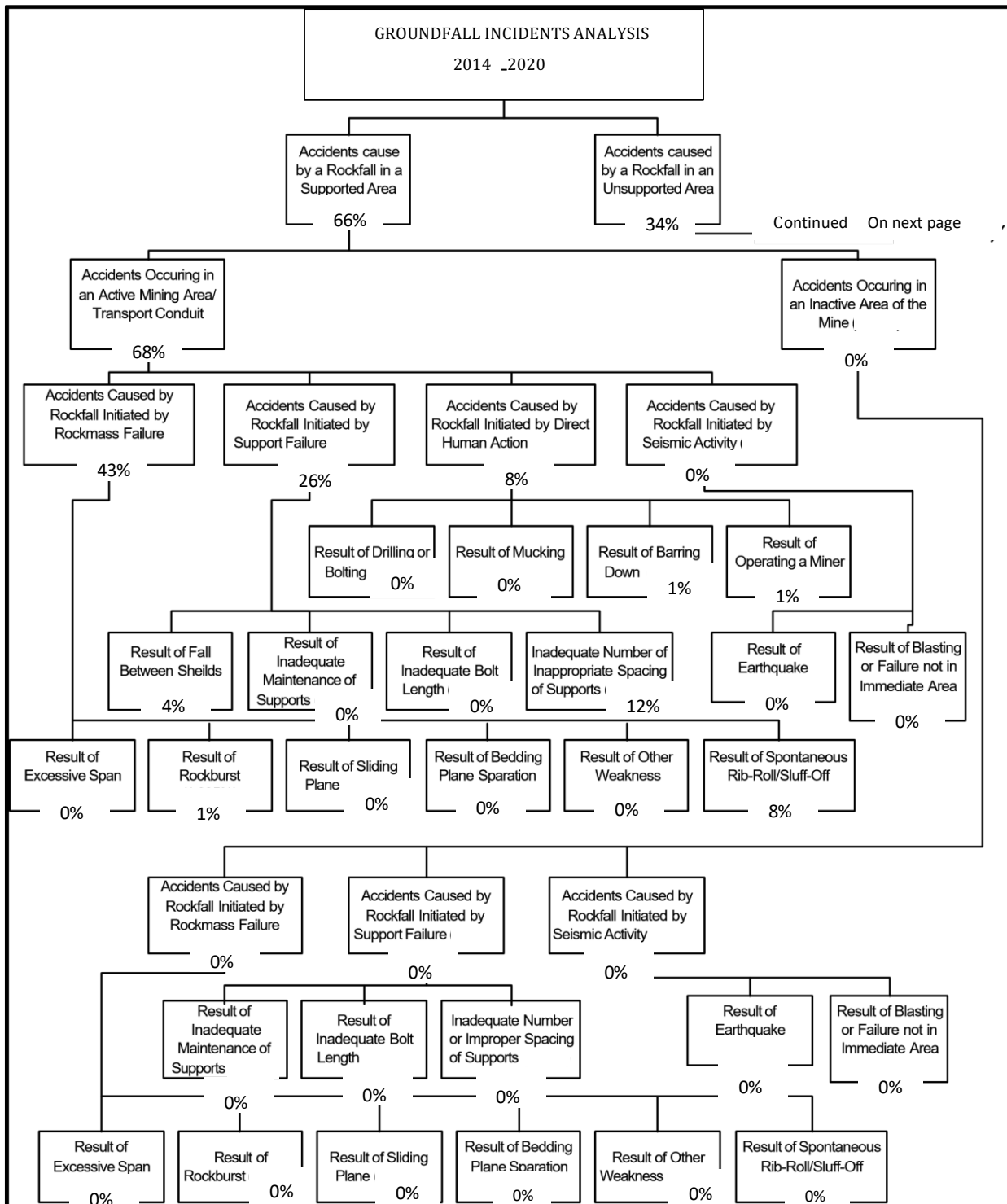
Besides the engineering properties of the local rocks, the geological structures inherent to these rocks has a great bearing on the safety and stability of the engineering excavations made in hard rock underground mines. Geotechnical mapping was employed to create a plan of the 3 South Section and an extract MRM Systems, and the observations below were established.

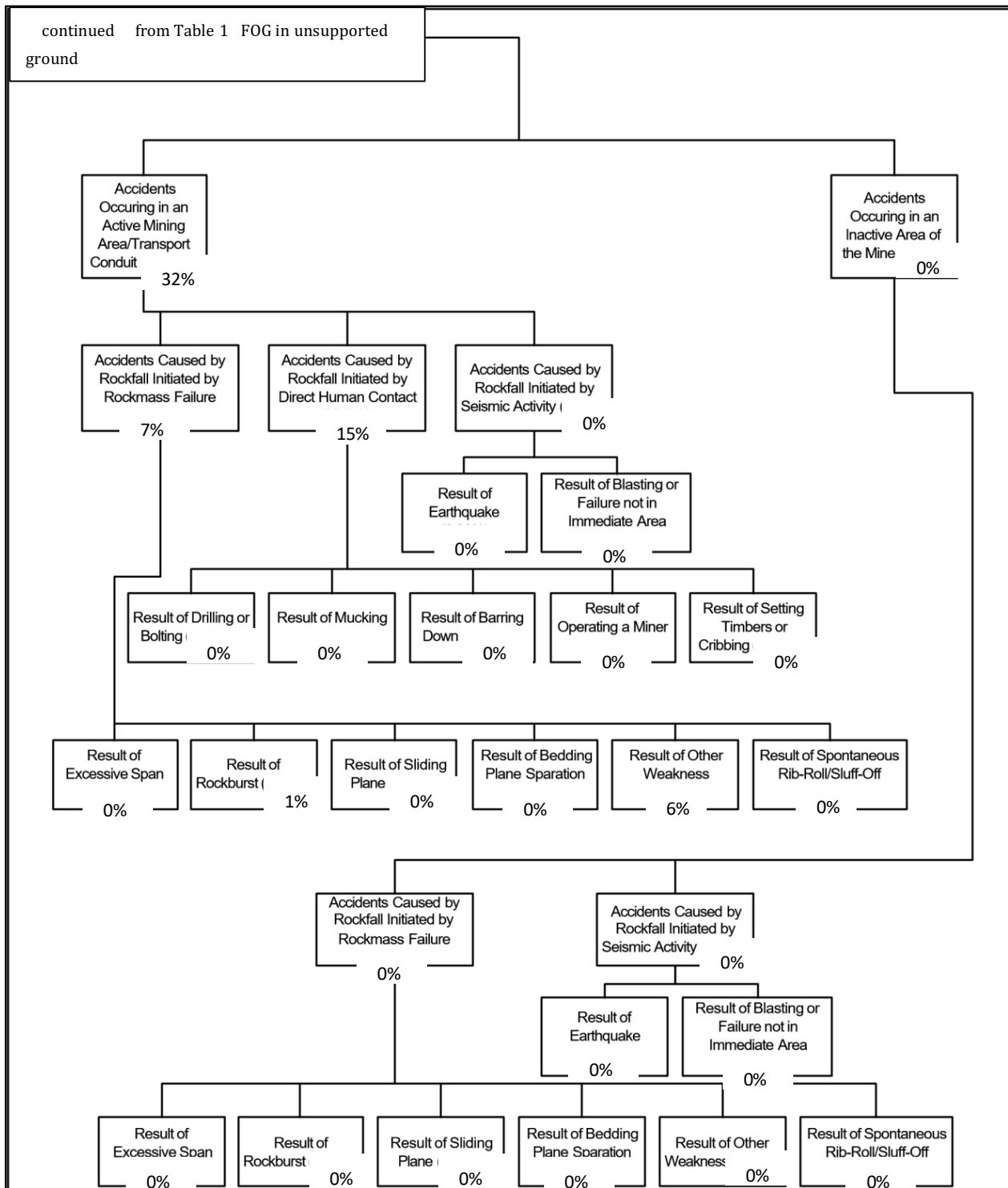
Two chief N-S steeply-dipping, 600 and two main E-W steeply-dipping, 400 joint sets intersecting the hanging and the sidewalls creating a possibly insecure wedges in both walls. The joint sets are intersected by dome structures creating blocky ground conditions, possibly compromising stability as well. A fault, 0.3m thick, extremely altered, mylonitised and brecciated plagioclase pyroxenite with talcose fault gouge exists in the foot wall with a friction angle of 15° and compromises pillar strength by up to 35%. N-S and E-W trending fault series exist, and they form planes on which rock movement has occurred leading to reef displacement. E-W trending dykes typically hard, fine-grained dolerite 0.003m and 0.04m occurring continuously in production panels on all walls.



Fig. 9. Pillar compromised by existence of dykes.

**Table 1.** Taxonomic analysis of fog statistics.





Jointed dykes creating blocky ground, irregular, large scale, and rough contacts were recorded. They render the area unstable and compromise pillar loading as the overall stiffness of the loading system affects the load transfer to pillars hence an untrue impression maybe assumed on pillar strength if the geologically motivated loading is unaccounted.

**Table 2. Geotechnical Data**

End	Peg	Ditance	Joint set No.	Orientation	Trace Length	Micro roughness	Macro roughness	Infill	Infill thickness	Fault/face
3SB1	5009	8.39	2+R	Fair	3-10m	Rough	Discontinuous	Hard	1-5mm	None
		15.53	2+R	Unfavourable	3-10m	Rough	Discontinuous	Hard	1-5mm	None
		22.77	2+R	Unfavourable	3-10m	Rough	Planar	Soft	> 5mm	d-EW
		-9.33	2+R	Very	10-	Rough	Planar	Hard	> 5mm	None
		-17.36	1+R	Very	10-	Smooth	Planar	Soft	1-5mm	d-EW
3SB2	5010	7.38	2+R	Unfavourable	3-10m	Rough	Planar	Hard	1-5mm	None
		13.33	3+R	Unfavourable	10-	Slickensided	Planar	Soft	1-5mm	d-EW
		21.66	2	Fair	3-10m	Smooth	Planar	Hard	1-5mm	d-EW
		-10.49	2+R	Fair	3-10m	Smooth	Planar	Hard	1-5mm	None
		-20.63	3+R	Unfavourable	10-	Smooth	Planar	Hard	1-5mm	d-EW
3SB3	4961	8.16	3+R	Unfavourable	10-	Rough	Planar	Hard	1-5mm	d & FEW
		16.25	2+R	Fair	3-10m	Slickensided	Planar	Soft	1-5mm	d-EW
		-9.45	2+R	Unfavourable	3-10m	Rough	Discontinuous	Hard	1-5mm	d-EW
		-17.79	3+R	Unfavourable	3-10m	Rough	Discontinuous	Soft	1-5mm	d-EW,
		8.45	3+R	Unfavourable	3-10m	Rough	Planar	Soft	1-5mm	d & FEW
3SB4	5047	18.63	2+R	Fair	3-10m	Smooth	Planar	Hard	1-5mm	d-EW
		27.13	2+R	Fair	3-10m	Smooth	Planar	Hard	1-5mm	d-EW
		-8.47	3+R	Unfavourable	10-	Rough	Discontinuous	Soft	1-5mm	none
		-18.09	2	Fair	10-	Smooth	Planar	Soft	1-5mm	d-EW
		10	2+R	Fair	3-10m	Rough	Discontinuous	Soft	1-5mm	d-EW
3SB5	5048	20.3	2+R	Favourable	10-	Rough	Planar	Hard	1-5mm	d-EW
		30.78	2+R	Favourable	3-10m	Smooth	Discontinuous	Hard	1-5mm	d & FEW
		41.4	2+R	Fair	10-	Rough	Discontinuous	Soft	> 5mm	d-EW
		9	1+R	Unfavourable	3-10m	Rough	Planar	Soft	> 5mm	d-EW
		18.24	2+R	Fair	3-10m	Rough	Planar	Hard	1-5mm	d-EW
3SB6	5068	27.42	2	Fair	3-10m	Rough	Planar	Hard	> 5mm	d-EW
		-9.55	2+R	Fair	3-10m	Smooth	Discontinuous	Hard	> 5mm	d & FEW

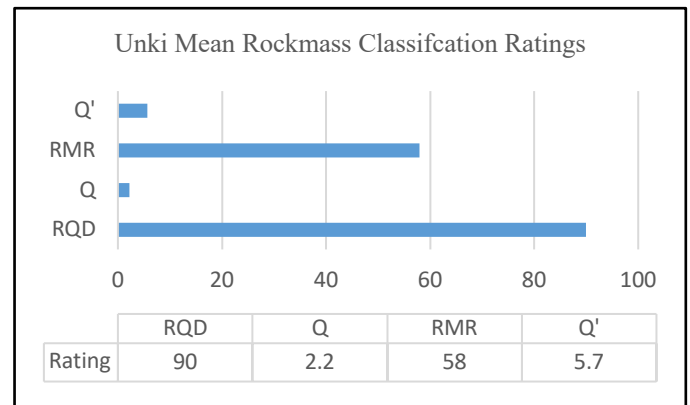
4.5 Rock mass classification

Table 2 presents the geotechnical data that was gathered during the field surveys of the section that was under study at Unki Mine.

From Table 2, the bulky of the joints can be characterized as planar and rough containing soft low friction clay infill 1mm to 5mm inclusive of chlorite or serpentine which significantly reduces their stiffness and shear strength and consequently that of pillars.

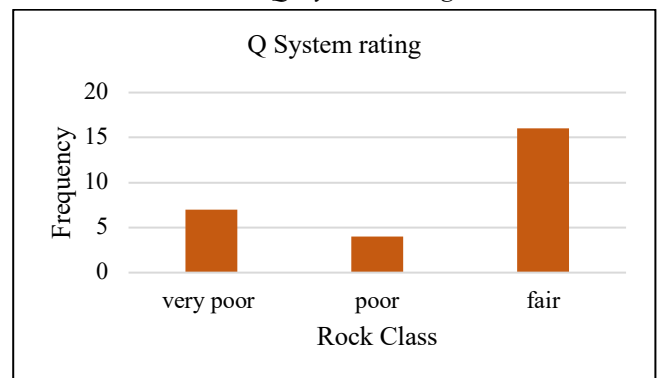
4.6 Rock Mass Classification Ratings

Figure 10 below summarizes the rock mass classification ratings for Unki as analyzed from the data collected during the field work.



**Fig. 10. Rock Mass Classification Rating Data**

4.7 NGI Geomechanics Q. System Rating



**Fig. 11. Q. Rating Rock Mass Classification**

Fig 11 makes it clear that the prevailing rock class conditions are poor based on the Q-System of rock mass classification. Deductions of the ratings for each parameter for the computation of the Rock Tunneling Quality Index (Q) were made at each interval in each panel in the section.

4.8 Rock Quality Designation (RQD)

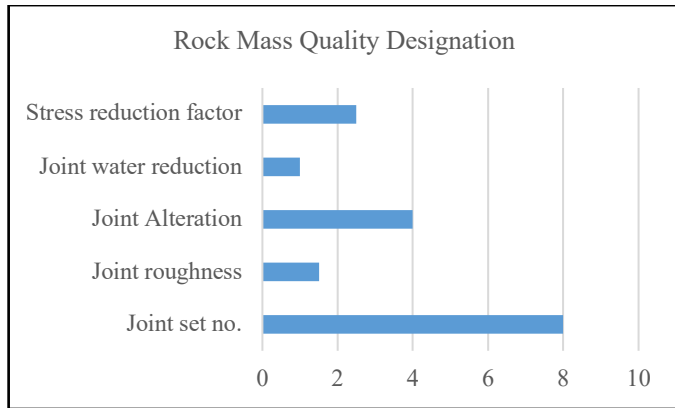


Fig. 12. Rock quality designation

The Palmström's relationship for exposure mapping  $RQD = 115 - 3.3 J_v$  was used for computations of RQD at each interval in stope panels and to facilitate the computation of a mean RQD of 90. Major joint sets were N-S trending of 400 to 500 dip angles and an E-W trending 600 dip joint sets. These joint sets often intersected with hanging wall shear zones creating steeply dipping wedges and on intersecting with the footwall fault on pillars they introduced scaling to pillars. The mode of the joint set number was therefore 2 + 6 for random jointing.

The modal joint roughness rating was 1.5 showing that most joints were both planar in terms of macro roughness and rough in terms of micro roughness. The bulky of the joints within the section under scrutiny had infill thickness between 1mm and 5mm either soft or low-friction clays inclusive of kaolinite, mica, Chlorotic talc and gypsum. Consequently, the rating was found to be a 4. The water reduction factor was put at 1 considering of the joint sets that were within the section that was under study were dry. Existing within a range of 200m to 300m from the surface, the ore body is generally characterized by low stress thus a factor of 2.5 was reached.

4.9 Bieniawski's Rock Mass Rating

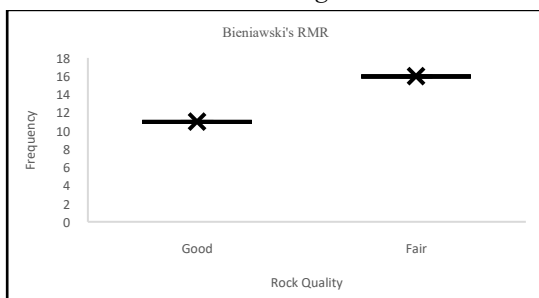


Fig. 13. : Bieniawski's RMR for Unki Mine rocks

An analysis of figure 13 above indicate that the general conditions of the mine section that was under scrutiny has Fair rock based on the Geomechanics RMR System with a mean rating of 57. The modal RQD rating sat at 20 for RQD falling within the range of 100-90.

4.10 Laubscher's Mining Rock Mass Rating System

The MRM ratings per bord in the section were averaged to give a rating of 62.4. RQD and UCS had modal ratings of 14 and 18 respectively.

4.11 Joint rating

The bulk of the joints in the section exhibited to be straight hence earning a large-scale joint rating of 75%. While on a micro scale most joints were rough and planar leading to a 65% rating, 75% and 85% for fill and alteration respectively. Mean joint condition rating was found to be 16.4.

The mean spacing rating for the whole section sat at 13.7. For various field measurements from the section, the joint spacing graph was employed to decide the ratings. For instance, measurements from the 3 South Bord 1 with 2 joint sets (spacing 210mm and 540mm) was computed as below.

$$J_s = 25 \times 0.72 \times 0.78 = 14 \tag{16}$$

4.12 Design Rock Mass Strength (DRMS)

Given there was generally 2 joint sets per interval, the modal joint orientation adjustment for the mine section sat at 85% and the adjustment for weathering was put at 100% since the weathering was fresh. Design mining height is 2m and the recorded peak reached 2,45 hence the blasting adjustment came to 82%. Thus, the DRMS, also k value for MRMR is 53 MPa. The computed k value is 7% less the k value of 57.33 MPa (1/3 \* UCS) used for existing pillar design hence the pointing out to the over valuation of existing pillar strength.

4.13 Pillar Performances

This was chiefly prompted by the presence of the footwall fault in the section. The fault; 0.35m average thickness creating an undercut for side wall failure under gravity. Joint sets, 600 dip also cut through the pillars intersecting with the faults and prompted stress fracturing. In some circumstances pillar edges peel-off in well-defined planes where the failure was prompted by the shear movement along dykes.



Fig. 14. Pillar failure as prompted by foot wall faults.



Fig. 15. Pillar failure influenced by dykes.

4.14 Progressive Slabbing

Predominantly, tress induced progressive pillar failure detected characterized by spalling slabs off the pillar walls. Heavily loaded pillars display unstable signs preceding complete failure. When pillar stress gradually surges, rock fracturing and spalling will be visible on pillar edges. Figure 16 and Figure 17 below are true depiction of this as at the Mine.



Fig. 16. Preliminary Phases of pillar slabbing



Fig. 17. Hour glassing progressive pillar slabbing.

The following set of figures from 18 to figure 23 summarizes the results that were obtained from the lab tests on various engineering properties of the rock samples from Unki Mine. From this data, more descriptive statistics for the hanging wall, footwall and ore were driven. The results are also critical in carrying out an appraisal on the safety of the existing support design and proposing new modifications.

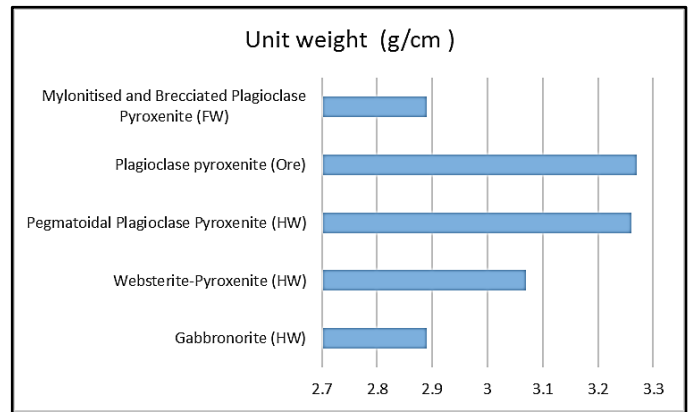


Fig. 18. Unit weight

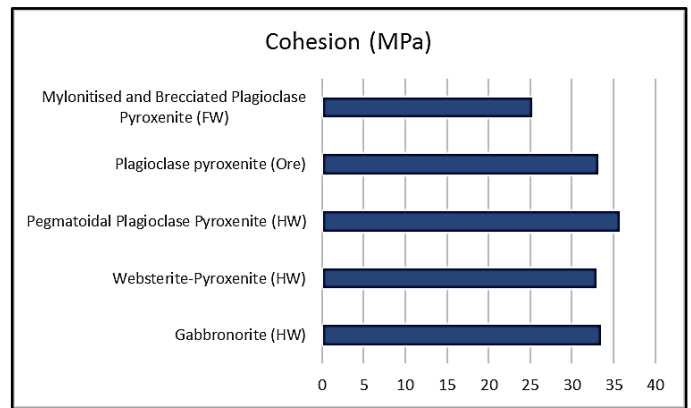


Fig. 19. Cohesion laboratory

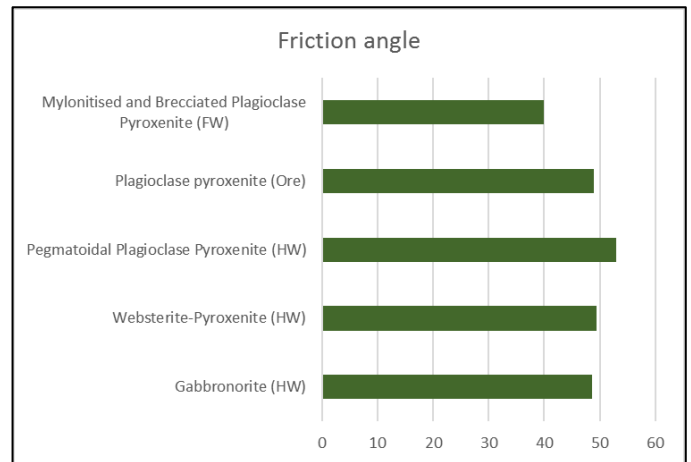


Fig. 20. Friction Angle laboratory

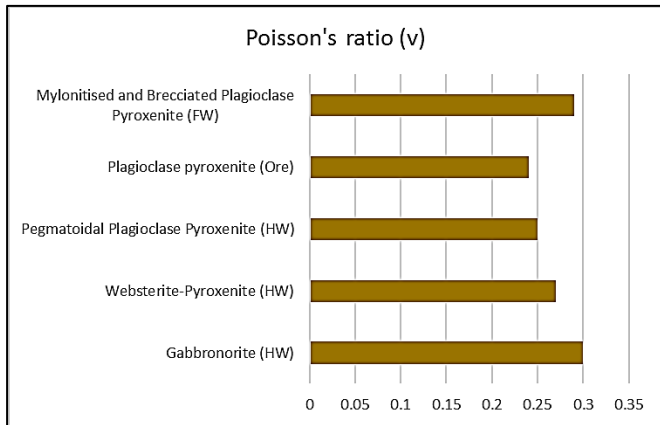


Fig. 21. Poisson's Ratio

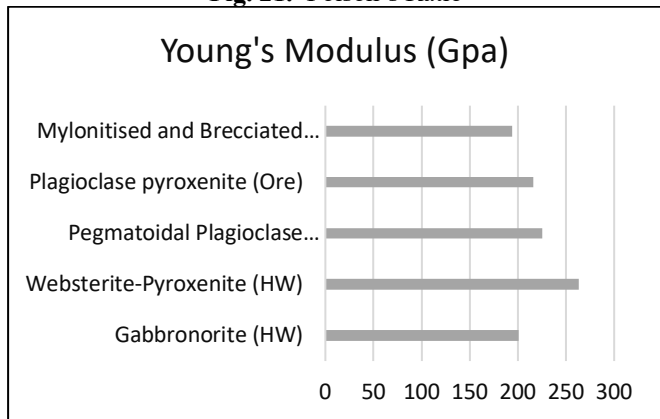


Fig. 22. Young's modulus

The overall analysis from figure 18 to figure 23 indicates that the immediate hanging wall comprises of a stratum of pegmatoidal pyroxenite, consequently forming a tensile zone. The Pegmatoidal pyroxenite stratum occurrence ranges between 0.5 m and 1.9 m above the BMSZ. It possibly may possess possible parting as influenced by its large grain sized particles enabling splitting along crystal cleavage planes.

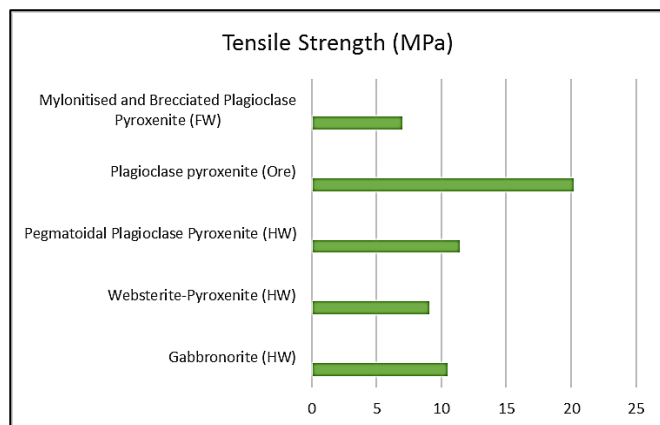


Fig. 23. Tensile Strength

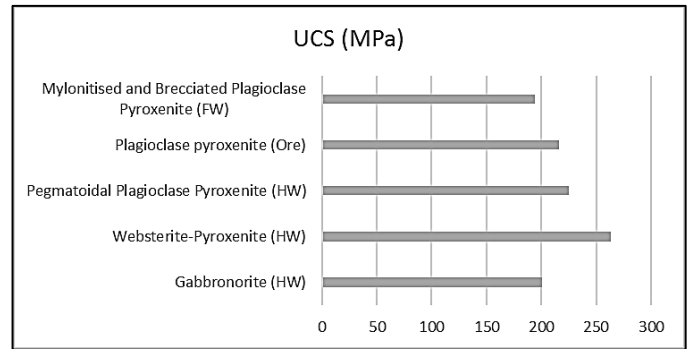


Fig. 23(a). UCS

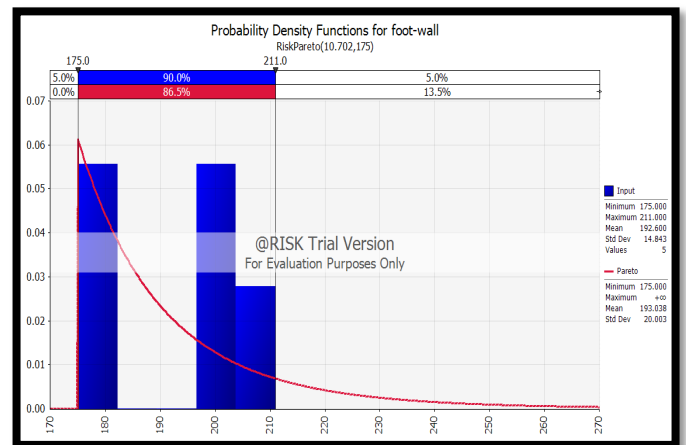


Fig. 24. Probability Density function HW UCS

On the contrary, the ore comprises of a plagioclase pyroxenite stratum within which mining takes place thus forming the bulk of the pillars left standing. This zone is therefore characterized by hard and tough rock up to 216 MPa UCS on average as illustrated by figure 24 however plagioclase pyroxenite is extremely jointed thus compromising the rock mass strength and the possible stable stope span.

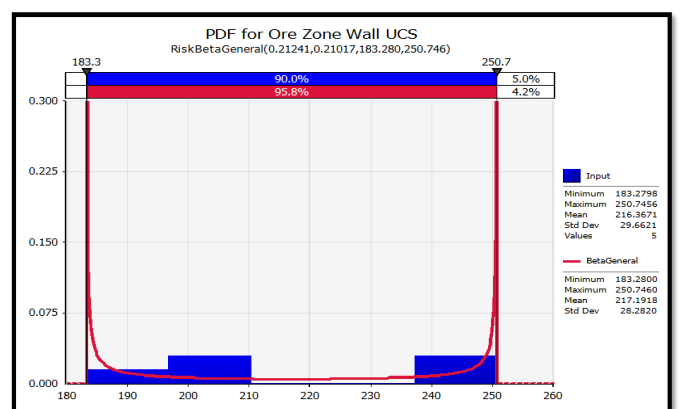


Fig. 25. Ore UCS Probability Density function

The foot wall comprises of a shear zone of chloritic talc about 0.3m thick. The mean Uniaxial Compressive Strength is just above 190 MPa, the least just below 185 MPa and peak UCS of 205 MPa as shown in Fig 25.

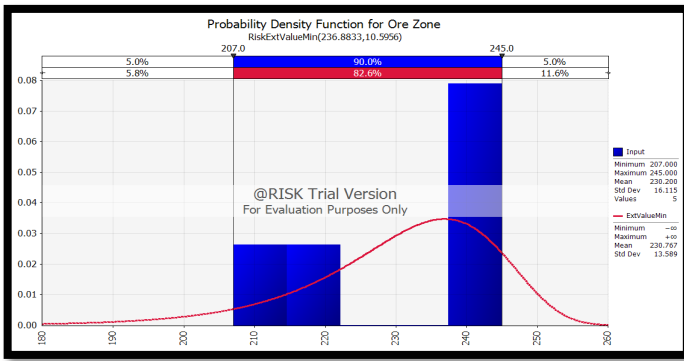


Fig. 26. Footwall UCS Probability Density function Optimal Span stability

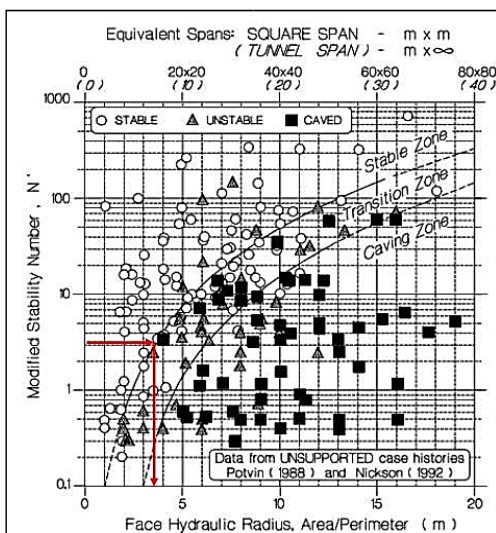


Fig. 27. Modified stability graph stable span without support

The mean  $Q'$  per interval recorded was 5.73, modal rating for the rockmass stress factor  $A=1$  was adopted; thus no stress impact is predictable between 150m to 200m depths. True face to joint angle mean was 35o, a joint orientation adjustment  $C=0.2$  was adopted. The average  $H/W$  inclination was 10; Gravity adjustment  $C=2.1$  was adopted. The mean modified stability number  $N'$  was established to be 3.1 and was employed in the modified stability chart in Figure 27 above and a hydraulic radius of 3.6m was adopted hence a stable stope span of 7.2m without support.

4.15 Q-System

The Q-index results were employed to govern the stable span without support together with the subsequent stand-up time. The mean Q rating  $QAve = 2.23$  was employed as illustrated in Fig 28.

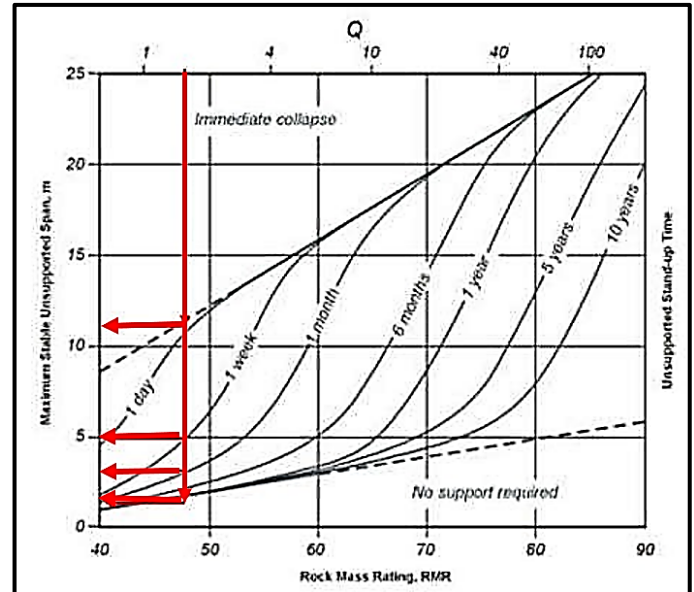


Fig. 28. Stable Span based on the Q-System

The figure above clearly shows an extreme stable span of 11m, and 24 hrs. stand up time hence artificial support will be necessary to be administered within a day. For a stand up of 7 days, the stable span should not exceed 5m: and for 30 days, 3m and 1m for totally unsupported ground.

5. CONCLUSION

The ultimate objective of this study was to ensure a robust design of support systems at Unki Mine that would eventually reduce the risks associated with rock engineering excavations. Findings from the study and its analysis established the following conclusions.

1. On the fore is the fact that hanging wall instability at Unki Mine are predominantly governed by geological and span attributes.
2. The computed k value is 7% less the k value of 57.33 MPa ( $1/3 * UCS$ ) used for existing pillar design hence pointing out to the over valuation of existing pillar strength.
3. Figures 4.2 and 4.3 on analysis of FOS and its relationship with recovery and Pillar W/H ratio shows that over-break has a huge impact on the span stability hence the effect of the ANFO employed by Unki Mine need to be reviewed for an alternative explosive that ensures recovery within 80% range to ensure that the FOS is maintained above 1.6. A decrease in FoS increases the probability of failure, hence it is also important to devise a pillar support system that is less prone to effects of over-break since the ground conditions are poor.

The following recommendations were highlighted following the taxonomic analysis on the FoG statistics, analysis of Unki geological structures and rock mass characteristics as well as the optimal design for the rock engineering excavations. The taxonomic analysis on FOG statistics proved that rock mass failure resulted in just below 50% of FOG at the mine,

support failure caused 26% FOG incidents and human interactions accounted for the extra 24%. It is therefore recommended that the mine increases efforts to detect rock mass abnormalities and human interactions with support systems is critical in reinforcing the rock engineering risk management systems. In addition, to further significantly reduce the rock engineering risks in underground excavations at Unki Mine, the analysis from the modified stability graph leads to the suggestion that an unsupported span of 7.4m is recommendable instead of 12m. Adopting an effective mining height of 2m and a  $k_{value} = DRMS = 53.2$  a pillar width of 7m is proposed along strike and 5m along dip. Ventilation holings measure 5m (dip) by 7.5m (strike) yielding the required FOS of 1.6 and no pillar failure likelihoods.

## REFERENCES

- [1] Abbas, S. & Konietzky, H., 2015. Rock mass classification systems. pp. 1-26.
- [2] Bieniawski, Z. T., 1989. Engineering rock mass classification: a complete manual for engineering and geologist in mining, civil and petroleum engineering. John Wiley & Sons.
- [3] A.T.M Farid (2019) Modified Value of Rock Quality Designation Index RQD in Rock Formation
- [4] Bieniawski, Z. & Hawkes, L., 1978. Suggested methods for determining tensile strength of rock material. International journal of rock mechanics and mining sciences, I(5), pp. 99-103.
- [5] Bigby, O. N., 1997. Developments in British rock bolting technology.
- [6] Deeren, D. W., 1989. Rock Quality Designation (RQD) after Twenty Years: Deere (DON U) CONSULTANT GAINESVILLE FL..
- [7] Dhandad, I., 2005. First Indian Mineral Congress and Technological Exhibition: Allied Publishers.
- [8] Eberhardt, E., 2003. Rock slope stability analysis- Utilisation of advanced numerical techniques. Geological Engineering\ Earth and Ocean Sciences, I(1), pp. 1-30.
- [9] Fairhurst, C. & Hudson, J., 1999. Draft ISRM suggested method for the complete stress-strain curve for intact rock in uniaxial compression. International journal of rock mechanics and mining sciences, II(36), pp. 279-289.
- [10] Haile, A. T. & Jager, A. J., 1995. Rock mass condition, behaviour and seismicity in mines of the Bushveld igneous complex, Johannesburg, South Africa.
- [11] Laubscher, D. H., 1990. A geomechanics classification system for the rating of rock mass in mine design. The journal of the South African Institute of Mining and Metallurgy, Volume 90, pp. 257-273.
- [12] Laubscher, D. H. & Taylor, H. W., 1976. The importance of geomechanics classification of jointed rock masses in mining operations. In proceedings of the Symposium on Exploration for Engineering, November, Volume 1, pp. 119-128.
- [13] Lou, J., Haycocks, C., Karmis, M. & Westman, E., 1988. A critical overview of U.S rock bolting practices, Aachen Germany: Third International Symposium, roof bolting in mining.
- [14] Mandingaisa, O., 2014. Code of practice to combat rockfall and rockburst accidents, Shurugwi: Unki Mine.
- [15] Mark, C., 1998. Comparison of ground conditions and ground control practices in the United States and Australia, Morgantown.
- [16] Fairhurst, C. & Hudson, J., 1999. Draft ISRM suggested method for the complete stress-strain curve for intact rock in uniaxial compression. International journal of rock mechanics and mining sciences, II(36), pp. 279-289.
- [17] Mark, C., 2001. Overview of ground control research for underground coal mines the United States, Turkey.
- [18] Bieniawski, Z. T., 1989. Engineering rock mass classification: a complete manual for engineering and geologist in mining, civil and petroleum engineering. John Wiley & Sons.
- [19] Obert, L. & Duvall, W. I., 1967. Rock mechanics and the design of structures in Rock: John Wiley and Sons.
- [20] O'Connor, D., van Vuuren, J. & Altounyan, P., 2002. Measuring the effect of bolt installation practice on bond strength for resin anchored rockbolts.
- [21] A.T.M Farid (2019) Modified Value of Rock Quality Designation Index RQD in Rock Formation
- [22] Peng, S. S., 1998. Roof bolting adds stability to weak strata: John Wiley and Sons.
- [23] Portvin, Y., 1988. Empirical open stope design in Canada, Ph.D. thesis, University of British Columbia.
- [24] Rocscience, 2007. Roclab software user manual.
- [25] Stacey, T. & Gumede, H., 2008. Evaluation of risk of rock fall accidents in gold mines stopes based on measurement joint data. The Southern African Institute of Mining and Metallurgy, I(1), pp. 345-350.
- [26] A.T.M Farid (2019) Modified Value of Rock Quality Designation Index RQD in Rock Formation
- [27] Tully, D. M., 1987. The application of scale models in the design of rockbolting system for mine roadways: 28 U.S Symposium on Rock Mechanics.
- [28] Van der Merwe, J. N., 1989. A probabilistic approach to the design of coal mine roof support systems, Johannesburg: SANGORM Symposium.
- [29] Van der Merwe, J. N., 1998. Practical coal mining strata control. A guide for managers and supervisors at all levels., Johannesburg.
- [30] A.T.M Farid (2019) Modified Value of Rock Quality Designation Index RQD in Rock Formation
- [31] Laubscher, D. H. & Taylor, H. W., 1976. The importance of geomechanics classification of jointed rock masses in mining operations. In proceedings of the Symposium on Exploration for Engineering, November, Volume 1, pp. 119-128.